

ROTATION CURVES OF URSA MAJOR GALAXIES IN THE CONTEXT OF MODIFIED NEWTONIAN DYNAMICS

R. H. SANDERS AND M. A. W. VERHEIJEN

Kapteyn Astronomical Institute, Postbus 800, 9700 AV Groningen, The Netherlands

Received 1997 December 18; accepted 1998 March 20

ABSTRACT

This is the third in a series of papers in which spiral galaxy rotation curves are considered in the context of Milgrom's modified dynamics (MOND). The present sample of 30 objects is drawn from a complete sample of galaxies in the Ursa Major cluster, with photometric data from Tully et al. and 21 cm line data from Verheijen. The galaxies are roughly all at the same distance (15 to 16 Mpc). The radio observations are made with the Westerbork Synthesis Array, which means that the linear resolution of all rotation curves is comparable. The greatest advantage of this sample is the existence of K' -band surface photometry for all galaxies; the near-infrared emission, being relatively free of the effects of dust absorption and less sensitive to recent star formation, is a more precise tracer of the mean radial distribution of the dominant stellar population. The predicted rotation curves are calculated from the K' -band surface photometry and the observed distribution of neutral hydrogen using the simple MOND prescription, in which the one adjustable parameter is the mass of the stellar disk or the implied mass-to-light ratio. The predicted rotation curves generally agree with the observed curves, and the mean M/L in the near-infrared is about 0.9 with a small dispersion. The fitted M/L in the B -band correlates with $B-V$ color in the sense predicted by population synthesis models. Including earlier work, about 80 galaxy rotation curves are now well reproduced from the observed distribution of detectable matter using the MOND formula to calculate the gravitational acceleration; this lends considerable observational support to Milgrom's unconventional hypothesis.

Subject headings: galaxies: clusters: individual (Ursa Major) — galaxies: kinematics and dynamics — gravitation

1. INTRODUCTION

The rotation curves of spiral galaxies, as observed in the 21 cm line of neutral hydrogen, provide, in many cases, an accurate determination of the radial force distribution in regions of very low gravitational acceleration ($< 10^{-8}$ cm s $^{-2}$). Therefore, these data are ideal for testing alternatives to dark matter, such as Milgrom's proposed modified Newtonian dynamics (MOND), which posits that the discrepancy between the true gravitational force and the Newtonian force appears at low accelerations. As a theory of gravity or inertia, MOND predicts the precise form and amplitude of a rotation curve from the observed radial distribution of detectable matter (stars and gas) in a spiral galaxy, often with only one adjustable parameter, the mass-to-light ratio of the stellar disk (Milgrom 1983a, 1983b).

In two previous papers (Begeman et al. 1991, hereafter Paper 1; Sanders 1996, hereafter Paper 2), a sample of 33 spiral galaxies with published rotation curves was considered in the context of MOND. The 11 galaxies considered in Paper 1 were highly selected to meet certain strict criteria: the galaxies were rich in neutral hydrogen, the distribution and velocity field of the neutral gas was smooth and symmetric, the observed 21 cm line rotation curves extended far beyond the visible disk, and the galaxies were closer than 1000 km s $^{-1}$, in order to achieve high linear resolution and a large number of independent points along the rotation curve. In Paper 2 these criteria were relaxed to include an additional 22 galaxies with published 21 cm line rotation curves (as of 1996), but selection was still essentially based on H I richness and extent. For the combined samples of Papers 1 and 2, it was demonstrated that in most cases the observed rotation curve was predicted in detail from the observed light and gas distributions using the

simple MOND prescription. Moreover, the range of fitted values of M/L was astrophysically plausible and consistent with population synthesis models.

In the present paper, this work is extended to a new complete and homogeneous sample of spiral galaxies in the Ursa Major cluster. The sample has been previously considered in terms of the distribution by surface brightness (Tully & Verheijen 1997), but until now, the dynamics of these galaxies has not been discussed in the published literature. The important aspect of this sample is that it is optically selected (Tully et al. 1996). All galaxies in the Ursa Major cluster brighter than a specified limiting magnitude are considered, although the final sample is weighted against gas-poor systems because the rotation curves are determined from 21 cm line observations made at the Westerbork Radio Synthesis Telescope (Verheijen 1997). All sample galaxies have been imaged in the K' band (2.2 μ m) by Tully et al. (1996). Therefore, this sample is distinguished from the previous samples by its primary selection criterion and by its homogeneity; rotation curves of consistent and sufficient linear resolution are combined with near-infrared surface photometry in a data set that is well suited to the purpose of this work.

The previous combined sample of 33 field galaxies (Paper 2) was very inhomogeneous, the 21 cm line observations being carried out at either Westerbork or the VLA with differing angular resolutions and sensitivities. Considering the distance range covered by the sample (from 0.8 to 80 Mpc), the actual linear resolution of the neutral hydrogen observations varied between about 50 pc and 5 kpc. The 21 cm line data were taken by different observers using different methods of analysis. The photometry was quite inhomogeneous; in most cases this was CCD photometry, but

for several objects only older photographic photometry was available. The photometry was typically, but not always, in the B band, which is less reliable than redder bands as a tracer of the true radial distribution of the dominant stellar population, subject as it is to recent star formation and the effects of differential dust obscuration. Moreover, nine of these galaxies contained bulges or central light concentrations that, at least in the B band, yielded yet another fitting parameter: the M/L of the bulge component.

These problems are minimized in the Ursa Major sample. All galaxies are at roughly the same distance (taken to be 15.5 Mpc), which means that the linear resolution of the 21 cm line observations is similar in all cases (typically, 0.75 kpc). The relatively low scatter in the observed Tully-Fisher (TF) relation implies a rather small distance dispersion. The observations are reduced in the same way, and the same method is applied in deriving the rotation curves from the line data (Verheijen 1997). One of the greatest advantages of this sample is that the radial distribution of the old stellar population is determined from near-infrared (K' -band) CCD photometry, which is free from the above-mentioned problems associated with the B band. The galaxies are generally of quite late morphological type, and the effects of a separate bulge component with a spheroidal shape and separate M/L are minimal. Indeed, the M/L in the near-infrared is probably similar for the disk and the presumably older bulge component.

It is important to bear in mind that this is an *optically* selected sample; these galaxies are not selected for H I richness or the large extent of the neutral hydrogen disks. In many of these objects the neutral hydrogen does not extend far beyond the optical disk into the region of low accelerations, where the discrepancy between the visible and classical dynamical mass is large. Both high and low surface brightness galaxies are present, as well as a range of morphological types. Overall, this must be considered an advantage; it cannot be argued that these galaxies were picked as cases particularly favorable to analysis in terms of MOND. Moreover, the range of objects and accelerations probed illustrates some significant general characteristics of the mass discrepancy in spiral galaxies.

However, this complete and homogeneous sample is not completely free of problems. Because it is an optically selected sample, in a number of these objects the H I mass is low and its distribution is patchy—not ideal for derivation of a high-quality rotation curve. The distance to these galaxies is rather large compared to galaxies in the highly selected subsample of Paper 1. Combined with the fact that a number of the galaxies have a small angular size, the number of independent points on the measured rotation curve is, in several cases, quite low (less than five). The relatively poor linear resolution means that real structure in the rotation curve can be artificially smoothed (beam smearing). These galaxies are members of a cluster, albeit a loose cluster, and therefore quite a number of objects are interacting with near neighbors. This may complicate the interpretation of the neutral hydrogen velocity field as pure circular motion about the center of the galaxy. Taking these factors into account, the measured rotation curves, as tracers of the radial force law, are generally inferior to those of Paper 1, although the photometry is superior and the relative error in distance is smaller.

With these caveats in mind, we have carried out the MOND analysis on the galaxies in the Ursa Major sample.

This adds between 20 and 30 rotation curves (depending on internal selection criteria) to the total number considered in the context of this theory. The results are generally positive for modified dynamics; the predicted rotation curves agree with the observed curves and the range of implied M/L values is reasonable. In the K' band, the scatter in M/L is strikingly small: the mean M/L is about 1 in solar units, with a dispersion of 30%. This is entirely consistent with the scatter in the observed K' -band TF relation (Verheijen 1997); in the context of MOND, the only source of intrinsic scatter in the TF relation is the M/L , assuming planar gas disks in circular rotation. Below, we describe the sample, show the predicted and observed rotation curves, and discuss the implications for the hypotheses of modified dynamics and dark matter.

2. THE URSA MAJOR SAMPLE

Tully et al. (1996) identify 79 members of the Ursa Major cluster. The mean recession velocity is 950 km s^{-1} , with a dispersion of 150 km s^{-1} . Following Tully & Verheijen (1997), the distance to all galaxies in the sample is assumed to be 15.5 Mpc, although there is certainly a dispersion of 1 or 2 Mpc about this mean. There are 62 galaxies brighter than $M_B \approx -16.5$ that form a complete sample, and all of these have been imaged in the B , R , I , and K' bands (Tully et al. 1996). The H I velocity fields have been measured for most of these galaxies, but only 50 are sufficiently inclined (generally more than 45°) to be suitable for kinematic studies. Of these, 20 either are early types poor in H I, are strongly interacting with neighbors, or have fewer than five independent points along the measured rotation curve. Of the remaining 30, seven objects show kinematic evidence of velocity fields with significant deviations from circular motion due to interactions or nonaxisymmetric structure (bars). This leaves a sample of 23 objects that are free from obvious problems (Verheijen 1997).

The sample of 30 (including the kinematically disturbed systems) is listed in Table 1 with the observed properties. The objects are listed in column (1) along with the morphological type in column (2). Those systems previously designated by Verheijen (1997) as having a disturbed velocity field are indicated by an asterisk, and the “L” by the morphological type indicates that the galaxy is in the low surface brightness category (LSB), as defined by Tully & Verheijen (1997). The B - and K' -band luminosities are given in columns (3) and (4). The radial extent of the optical disk in the K' band, or, more specifically, the radius containing 80% of the near-infrared emission, is given in column (5), and the radial extent of the neutral hydrogen is given in column (6). The mass in neutral hydrogen is given in column (7), the rotation velocity at the outermost reliable point is given in column (8), and the centripetal acceleration in units of $10^{-8} \text{ cm s}^{-2}$ is given in column (9). We note that in several cases, the neutral hydrogen does not extend beyond the visible disk (e.g., NGC 3877 and NGC 3949); thus, these are not extended rotation curves, as considered in Papers 1 and 2. Moreover, for several galaxies the centripetal acceleration at the outermost point is higher than the previously determined value (Paper 1) of the MOND acceleration parameter ($a_0 = 1.2 \times 10^{-8} \text{ cm s}^{-2}$); therefore, in the context of MOND one would not expect a large discrepancy in these systems.

In several of the earlier type galaxies, the mean radial distribution of surface brightness does show evidence for a

TABLE 1
THE URSA MAJOR GALAXIES

Galaxy (1)	Type (2)	L_B ($10^{10} L_\odot$) (3)	$L_{K'}$ ($10^{10} L_\odot$) (4)	R_{80} (kpc) (5)	R_{H1} (kpc) (6)	M_{H1} ($10^{10} M_\odot$) (7)	V_{rot} (km s^{-1}) (8)	a ($10^{-8} \text{ cm s}^{-2}$) (9)
NGC 3726	SBc	2.65	3.56	7.5	28	0.48	162	0.30
NGC 3769*	SBb	0.68	1.27	4.4	32	0.41	122	0.15
NGC 3877	Sc	1.94	4.52	7.0	10	0.11	167	0.90
NGC 3893*	Sc	2.14	3.98	5.8	18	0.43	188	0.64
NGC 3917	Scd(L)	1.12	1.35	6.4	13	0.14	135	0.45
NGC 3949	Sbc	1.65	2.33	4.4	6	0.25	164	1.45
NGC 3953	SBbc	2.91	8.47	8.5	14	0.21	223	1.14
NGC 3972	Sbc	0.68	1.00	5.0	8	0.09	134	0.73
NGC 3992	SBbc	3.10	6.98	8.8	30	0.71	242	0.63
NGC 4010	SBd(L)	0.63	1.20	8.6	9	0.21	128	0.59
NGC 4013	Sb	1.45	4.96	5.3	27	0.22	177	0.38
NGC 4051*	SBbc	2.58	3.91	6.4	11	0.20	159	0.74
NGC 4085	Sc	0.81	1.22	3.5	5	0.10	134	1.20
NGC 4088*	Sbc	2.83	5.75	7.2	19	0.61	173	0.51
NGC 4100	Sbc	1.77	3.50	6.5	20	0.23	164	0.44
NGC 4138	Sa	0.82	2.88	3.0	16	0.11	147	0.44
NGC 4157	Sb	2.00	5.75	6.6	26	0.61	185	0.43
NGC 4183	Scd(L)	0.90	0.73	7.4	18	0.26	112	0.23
NGC 4217	Sb	1.90	5.29	6.9	14	0.19	178	0.73
NGC 4389*	SBbc	0.61	1.22	3.6	5	0.04	110	0.78
UGC 6399	Sm(L)	0.20	0.21	4.8	7	0.05	88	0.36
UGC 6446	Sd(L)	0.25	0.14	4.0	13	0.23	82	0.17
UGC 6667	Scd(L)	0.26	0.28	7.6	7	0.06	86	0.34
UGC 6818*	Sd(L)	0.18	0.12	3.6	6	0.08	73	0.29
UGC 6917	SBd(L)	0.38	0.42	5.8	9	0.15	110	0.44
UGC 6923	Sdm(L)	0.22	0.21	3.3	5	0.06	81	0.31
UGC 6930(i)	SBd(L)	0.50	0.40	3.7	14	0.24	110	0.23
UGC 6973*	Sab	0.62	2.85	1.7	7	0.13	173	1.39
UGC 6983	SBcd(L)	0.34	0.34	5.1	14	0.22	107	0.27
UGC 7089	Sdm(L)	0.44	0.21	5.1	8	0.09	79	0.25

central bulge component, or at least a central light concentration. However, we assume that in the near-infrared the difference in M/L between the bulge and disk is small, and the light distribution is not decomposed into separate bulge and disk components as in Papers 1 and 2 (this is justified by the results obtained below).

3. PROCEDURE AND RESULTS

The procedure for calculating and fitting MOND rotation curves to the observed curves is exactly as described in Papers 1 and 2. It is assumed that the azimuthally averaged radial profile of K' -band emission precisely traces the stellar mass distribution in an infinitesimally thin, axisymmetric disk; that is to say, we assume that there is no variation of the stellar M/L within a given galaxy, and the entire galactic mass, including any possible bulge component, is distributed in a thin disk. The gas mass distribution is assumed to lie in a thin disk and to be traced by the mean radial distribution of neutral hydrogen. The neutral hydrogen surface density is increased by a factor of 1.3 to account for the contribution of helium. Thus, given the distribution of observable matter, the Newtonian gravitational acceleration g_N is calculated in the usual way (see Begeman 1987).

The modified dynamics posits that the true gravitational acceleration g is related to the Newtonian acceleration as

$$\mu(g/a_0)g = g_N, \quad (1)$$

where a_0 is the MOND acceleration parameter and

$$\mu(x) = x(1 + x^2)^{-1/2}, \quad (2)$$

which is the commonly assumed form having the required

asymptotic behavior; i.e., gravity is Newtonian at high accelerations but is of the MOND form $g = (g_n a_0)^{1/2}$ at low accelerations (Milgrom 1983a).

The predicted rotation curve is determined by setting the true gravitational acceleration equal to the centripetal acceleration, as usual; i.e.,

$$V^2 = rg(r). \quad (3)$$

This is then fit in a least-square program to the observed rotation curve by adjusting the mass of the luminous stellar disk, the one free parameter of the fitting algorithm. The acceleration parameter is not allowed to be free, but is taken to be the value determined from the fits to the high-quality rotation curves of Paper 1; i.e., $a_0 = 1.2 \times 10^{-8} \text{ cm s}^{-2}$.

The distance is fixed at the value of 15.5 Mpc. Tully & Verheijen (1997) state that this distance is compatible with $H_0 = 85 \text{ km s}^{-1} \text{ Mpc}^{-1}$, given the complex velocity field in the local supercluster. Taking a mean radial velocity for the cluster of 1000 km s^{-1} , this distance would also be compatible with a smooth Hubble flow and $H_0 = 65 \text{ km s}^{-1} \text{ Mpc}^{-1}$. The value of a_0 derived in Paper 1 was based on galaxy distances estimated by taking $H_0 = 75 \text{ km s}^{-1} \text{ Mpc}^{-1}$; thus, it is not immediately evident that this same a_0 is consistent with the adopted distance to the Ursa Major cluster. Therefore, the MOND rotation curve fitting was repeated taking distance as a free parameter in addition to M/L . Eliminating ten extreme values (resulting from the attempt of the least-square program to accommodate all points on possibly beam-smear curves), the mean distance is found to be $15.2 \pm 3 \text{ Mpc}$. Thus, the assumed distance would seem to be consistent with the previously determined value of a_0 (and with $H_0 = 75 \text{ km s}^{-1} \text{ Mpc}^{-1}$).

It should be noted that in the context of MOND, the internal dynamics of a system is affected by the external acceleration field; i.e., when the external acceleration becomes comparable to or larger than a_0 , the internal dynamics is Newtonian, even though the internal accelerations may be smaller than a_0 (Milgrom 1983a, 1983c). Because the galaxies in this sample are members of a cluster, the magnitude of this external field effect should be considered. Given that the velocity dispersion of galaxies in the Ursa Major cluster is 150 km s^{-1} and that the characteristic size of the cluster is 1 Mpc, we find that the cluster acceleration on galaxies is typically on the order of $6 \times 10^{-3} a_0$; therefore, the individual galaxies may be considered as isolated systems, because the centripetal accelerations at the

outermost measured point of the rotation curve are typically more than 100 times greater than the cluster acceleration field (Table 1). Note that the low internal acceleration within the cluster would, in terms of MOND, imply a large conventional virial discrepancy. However, the dynamical timescale is longer than the Hubble time; the cluster is not virialized.

The results are given in Figure 1 and Table 2. As in Paper 2, the observed curve is shown by the points with error bars, the predicted MOND curve is shown by the solid line, the Newtonian rotation curve of the stellar disk corresponding to the MOND fit is shown by the dotted line, and the Newtonian curve of the gaseous disk is shown by the dashed curve. The observed rotation curves are determined

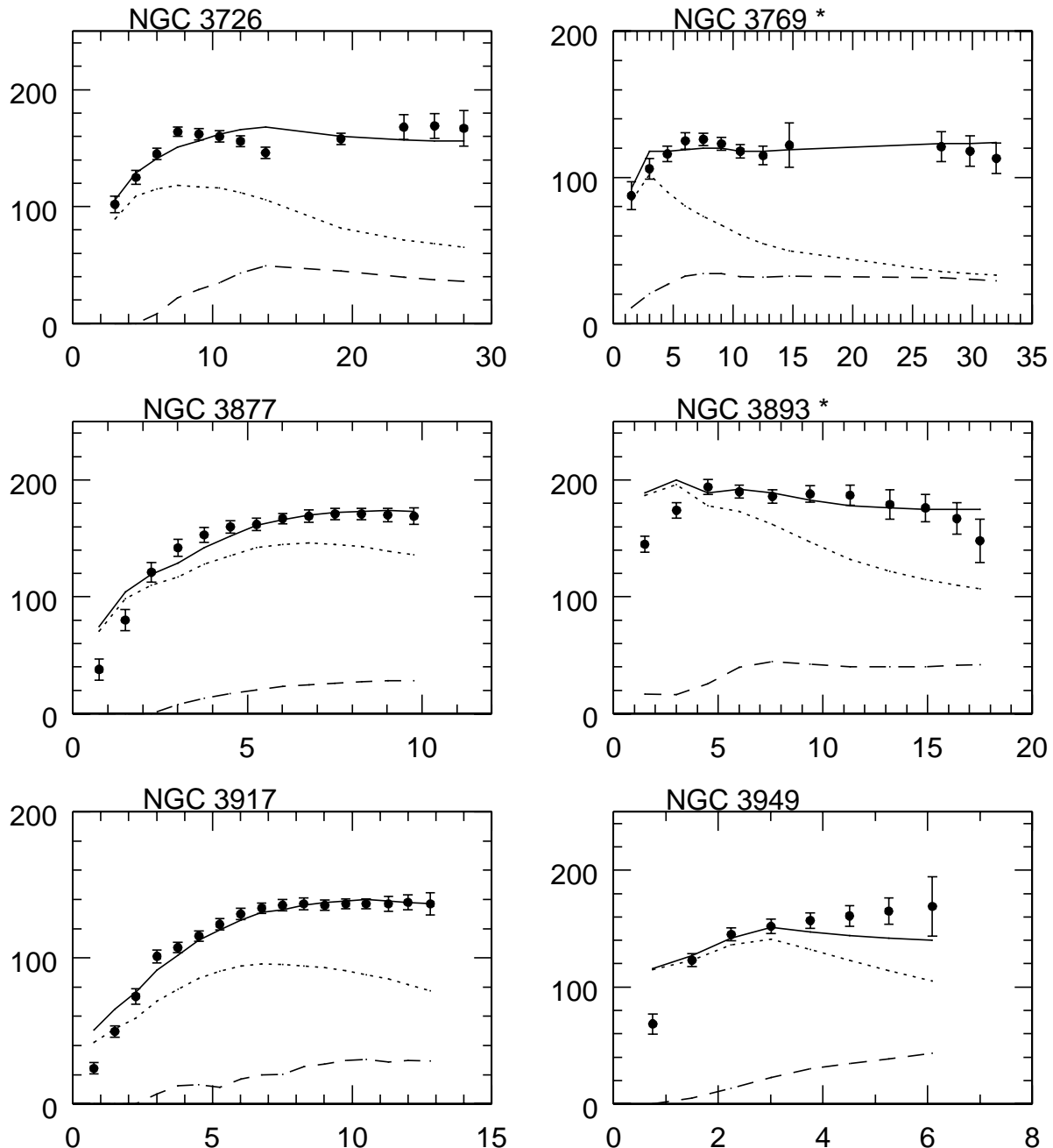


FIG. 1.—MOND fits to the rotation curves of the Ursa Major galaxies. In all cases, the radius (horizontal axes) is given in kpc and the rotation velocity in km s^{-1} . The points with error bars are the observations, and the solid line shows the rotation curve determined from the distribution of light and neutral hydrogen with the MOND formula. The other curves are the Newtonian rotation curves of the various separate components: *short dashed line*, rotation curve of the gaseous disk (H I plus He); *dotted curve*, that of the luminous disk. The free parameter of the fitted curve is the disk mass.

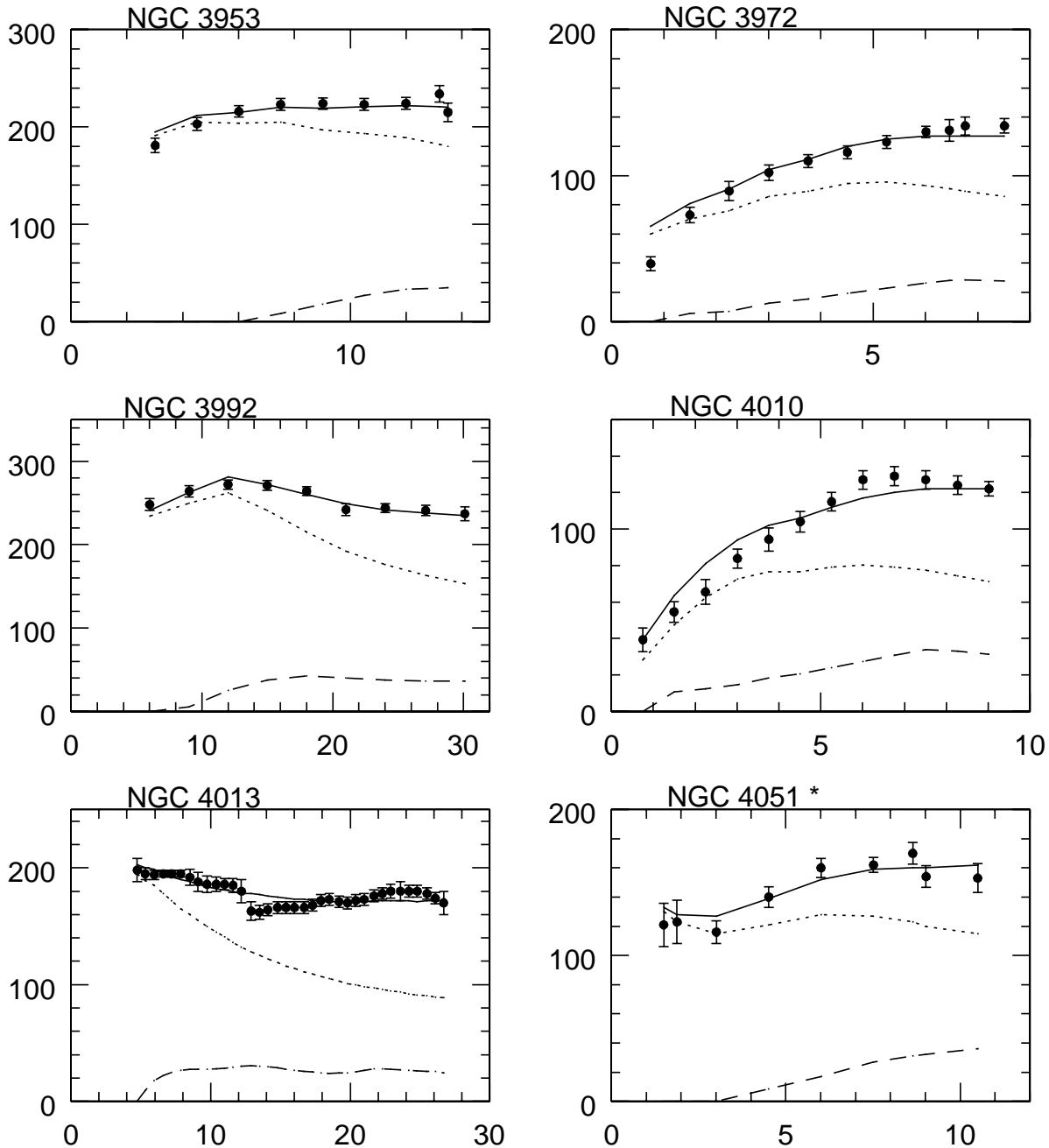


FIG. 1.—Continued

from the velocity field by the method of fitting tilted rings (see Begeman 1987), and interactively adjusted for beam-smearing effects, given the actual position-velocity diagrams in the inner regions. The error bars are also estimated by eye from the position-velocity diagrams and probably give a more realistic indication of the possible range of rotation velocity than do the formal errors returned by the ring-fitting program. As in Table 1, an asterisk indicates those systems with disturbed velocity fields.

Table 2 lists the fitted disk masses and errors for the sample galaxies. Also shown are the implied stellar mass-to-light ratios in the blue and near infrared (cols. [4] and [5]), as well as the total mass-to-light ratios in the near-infrared in column (6) (the total mass is the sum of the fitted stellar disk mass plus the observed gas mass). Because galaxy evolution models predict a relation between the mass-to-light

ratio in the various bands and the color of the stellar population, the extinction-corrected $B-V$ color is given in column (7) for those galaxies for which it has been determined (as tabulated in the Third Reference Catalog of de Vaucouleurs et al. 1991).

In general, the MOND rotation curves agree well with the observed curves, but in some cases the agreement is less than perfect. As it turns out, in most instances of serious disagreement, there are problems with the observed rotation curve or with its interpretation as a tracer of the radial force distribution. Several of these individual cases are discussed below.

NGC 3949.—Verheijen (1997) notes that this rotation curve has a considerable side-to-side asymmetry; it rises more steeply on the receding side than on the approaching

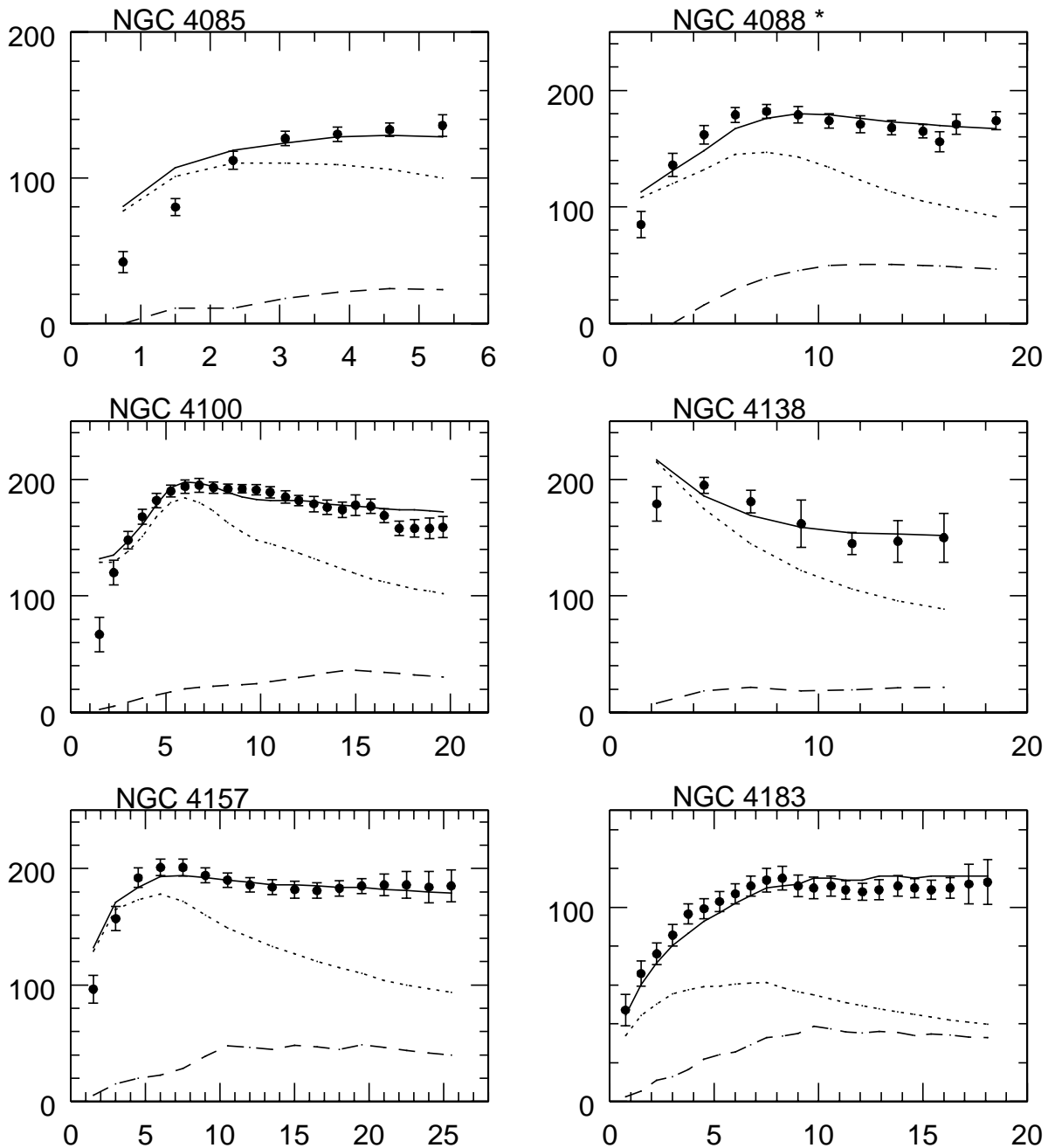


FIG. 1.—Continued

side, and there is a faint companion 1.5 to the north that may be interacting with this galaxy.

NGC 3992.—This barred system is the most luminous galaxy in the sample. Although the MOND rotation curve agrees well with the observed rotation curve, the required mass-to-light ratio of the stellar disk (2.2 in the near-infrared) is unusually large for this sample. This is also true for the various dark halo fits to the rotation curve (Verheijen 1997).

NGC 4389.—This system is strongly barred, and the neutral hydrogen is not extended but contiguous with the optical image of the galaxy. Verheijen (1997) points out that the velocity field cannot be interpreted in terms of circular motion and that the overall kinematics is dominated by the bar.

UGC 6446.—This low surface brightness, gas-rich galaxy has an asymmetric rotation curve in the inner regions; on the receding side it rises more steeply than on the approaching side. The MOND fit is much improved if the distance to this galaxy is only 8 or 9 Mpc instead of the adopted 15.5 Mpc. Such a possibility is consistent with the fact that this galaxy has the lowest systemic velocity in the sample: 730 km s^{-1} , which is 1.5σ below the mean of 950 km s^{-1} .

UGC 6818.—This is a dwarf galaxy that is probably interacting with a faint companion on its western edge (Verheijen 1997).

UGC 6930.—This is the one galaxy in the sample with an inclination of less than 45° ($i = 32^\circ$). It was included here because of its hydrogen richness ($M_{\text{HI}}/L_B = 0.5$) and its extremely regular velocity field.

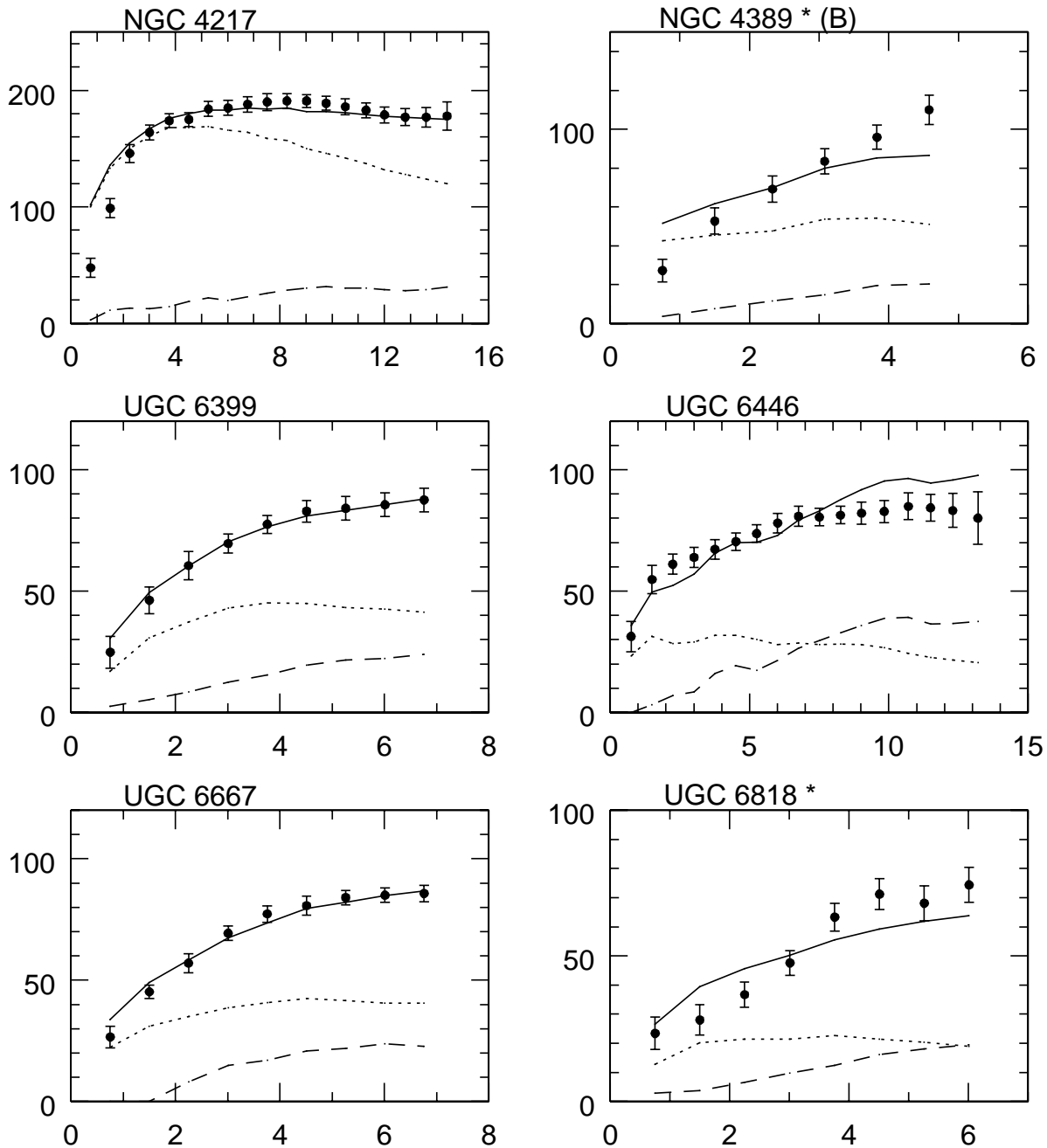


FIG. 1.—Continued

UGC 6973.—Verheijen (1997) notes that this galaxy is interacting with UGC 6962 to the northwest and that the H I disk is warped. Moreover, there is considerable evidence for vigorous star formation in the inner region, which is bright red and dusty. In the central regions, this is the reddest galaxy in the sample; in terms of central surface brightness, $\mu_0^B - \mu_0^{K'} = 6.47$ (Tully et al. 1996). This suggests that the K' band may be contaminated by dust emission and may not be a true tracer of the distribution of the old stellar population. The resulting calculated Newtonian rotation curve would be unrealistically declining as a result.

In a number of cases, the calculated rotation curve overshoots the observed rotation curve in the inner regions (e.g., NGC 3877, NGC 4085, and NGC 4217). These are highly inclined galaxies, and the true rotation curve could be

steeper than the one measured because of missing gas in the inner regions (H I holes). But there is an additional effect that may also be important. In calculating the Newtonian force from the observed light distribution, it was assumed that the stellar mass, including any possible bulge component, was distributed entirely in a thin disk. If the bulge component is spheroidal, this would then lead to an overestimate of the Newtonian force in the region of the bulge, given that the M/L of the bulge is taken to be the same as that of the disk. Therefore, in several cases it might be of interest to decompose the light distribution into a bulge and disk component. This would not add another fitting parameter, because in the near-infrared the M/L of the bulge and disk is probably quite similar, but it might well improve the fits in the inner regions.

In addition to the usual high surface brightness galaxies

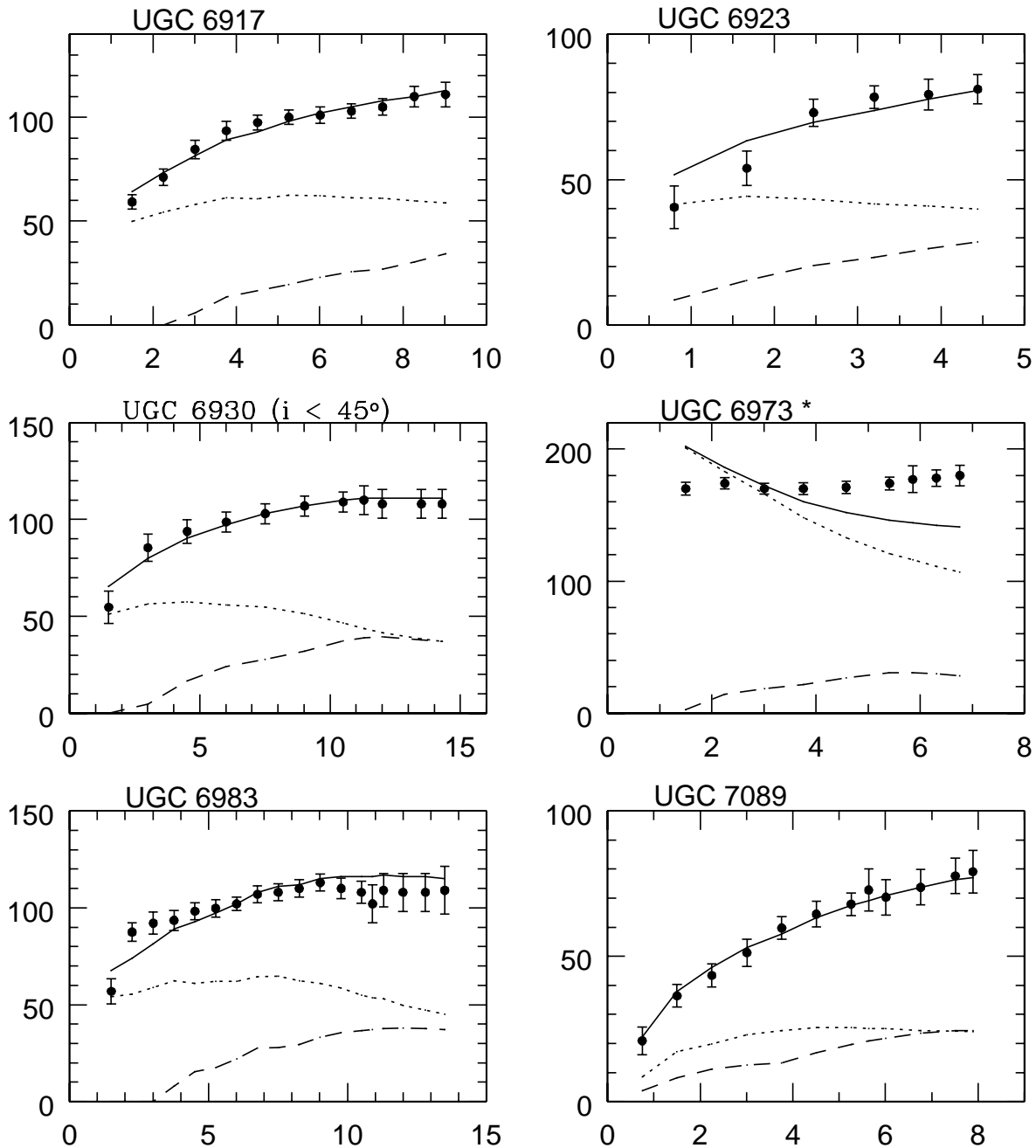


FIG. 1.—Continued

with extended rotation curves, this sample includes low and high surface brightness galaxies with measured rotation curves that do not extend far beyond the optical disk. Because of this, certain general trends are noticeable. For galaxies in which the acceleration at the last measured points of the rotation curve is comparable to a_0 (e.g., NGC 3877, NGC 3953, and NGC 4085), the discrepancy between the Newtonian rotation curve and the observed rotation curve is small—exactly as MOND predicts. For galaxies in which the gravitational acceleration at the last measured points is small in terms of a_0 (e.g., NGC 3769, NGC 4013, and NGC 4157, all low surface brightness galaxies), the observed discrepancy is large—again, exactly as MOND predicts. It is interesting that in the high surface brightness galaxies with extended rotation curves and a large discrep-

ancy in the outer regions (NGC 3769 and NGC 3992), Newton adequately explains the rotation curve in the inner regions and MOND takes care of the rest.

4. GLOBAL MASS-TO-LIGHT RATIOS IN THE NEAR-INFRARED AND BLUE

Figure 2 shows the distribution of mass-to-light ratios of the stellar disks in the near-infrared (Table 2, col. [5]) for the total sample of 30 galaxies. The shaded histogram applies only to the 23 objects without obvious disturbances in the velocity field (the objects not designated by an asterisk). It is evident that M/L_K is sharply peaked between 0.8 and 1.0; in the purified sample of 23, the mean M/L_K is 0.97 ± 0.36 . Excluding the most extreme case, the luminous

TABLE 2
THE MOND MASS AND THE IMPLIED M/L VALUES

Galaxy (1)	M_d ($10^{10} M_\odot$) (2)	\pm ($10^{10} M_\odot$) (3)	M_d/L_B (4)	M_d/L_K (5)	M_d/L_K (6)	$B-V$ (7)
NGC 3726	2.62	0.20	0.99	0.74	0.92	0.45
NGC 3769*	0.80	0.05	1.18	0.63	1.04	...
NGC 3877	3.35	0.17	1.72	0.74	0.77	0.68
NGC 3893*	4.20	0.27	1.96	1.06	1.19	...
NGC 3917	1.40	0.09	1.25	1.04	1.17	0.60
NGC 3949	1.39	0.16	0.84	0.60	0.73	0.39
NGC 3953	7.88	0.22	2.71	0.93	0.96	0.71
NGC 3972	1.00	0.08	1.47	1.00	1.12	0.55
NGC 3992	15.28	0.30	4.93	2.19	2.27	0.72
NGC 4010	0.86	0.07	1.37	0.72	0.94	...
NGC 4013	4.55	0.08	3.13	0.92	0.97	0.83
NGC 4051*	3.03	0.15	1.17	0.77	0.84	0.62
NGC 4085	1.00	0.13	1.23	0.82	0.92	0.47
NGC 4088*	3.30	0.18	1.16	0.57	0.71	0.51
NGC 4100	4.32	0.12	2.44	1.23	1.32	0.63
NGC 4138	2.87	0.25	3.50	1.00	1.04	0.81
NGC 4157	4.83	0.16	2.42	0.84	0.98	0.66
NGC 4183	0.59	0.035	0.65	0.81	1.27	0.39
NGC 4217	4.25	0.22	2.24	0.80	0.85	0.77
NGC 4389*	0.233	0.081	0.38	0.19	0.23	...
UGC 6399	0.207	0.008	1.04	0.99	1.33	...
UGC 6446	0.117	0.018	0.47	0.87	2.99	...
UGC 6667	0.249	0.022	0.96	0.89	1.17	...
UGC 6818*	0.040	0.013	0.22	0.33	1.18	...
UGC 6917	0.541	0.023	1.42	1.29	1.75	...
UGC 6923	0.164	0.030	0.75	0.78	1.11	0.42
UGC 6930	0.416	0.023	0.83	1.04	1.84	...
UGC 6973*	1.69	0.190	2.72	0.59	0.64	...
UGC 6983	0.565	0.036	1.66	1.66	2.51	...
UGC 7089	0.092	0.005	0.21	0.44	0.96	...

spiral NGC 3992, this becomes 0.92 ± 0.25 ; i.e., there is less than 30% scatter in the fitted near-infrared M/L .

In Paper 2 it was pointed out that there is a rough correlation between the MOND stellar mass-to-light ratio in the B band and the asymptotic rotation velocity: the more massive galaxies have a larger M_d/L_B . In Figure 3, which is a plot of M_d/L_B versus rotation velocity at the outermost measured point, this correlation is also evident for the galaxies in the present sample. The solid circles mark the 30

galaxies in the Ursa Major sample, and the open circles show the published sample of 33 field galaxies considered in Papers 1 and 2. The values for the Ursa Major galaxies range between 0.2 and 5, and there is a clear trend with rotation velocity of the form $M_d/L_B \propto V^3$. The overlapping of the two sets of points indicates the consistency of the

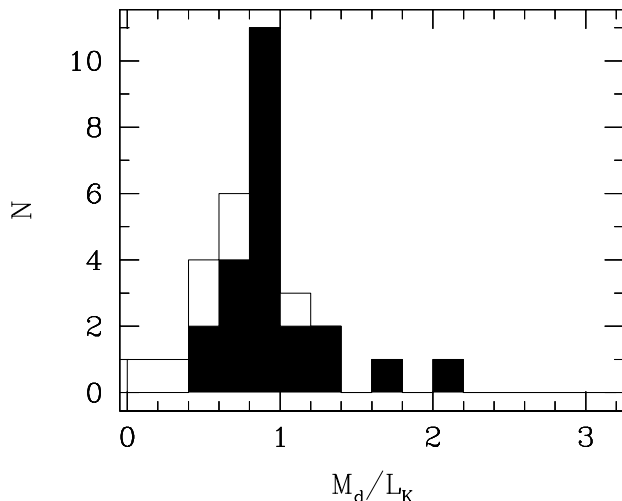


FIG. 2.—Distribution of the mass-to-light ratio in the near infrared, M_d/L_K , for the sample of 30 Ursa Major galaxies, where M_d is the mass of the stellar disk determined from the MOND fit. The shaded histogram is for the subsample of 23 galaxies with undisturbed velocity fields.

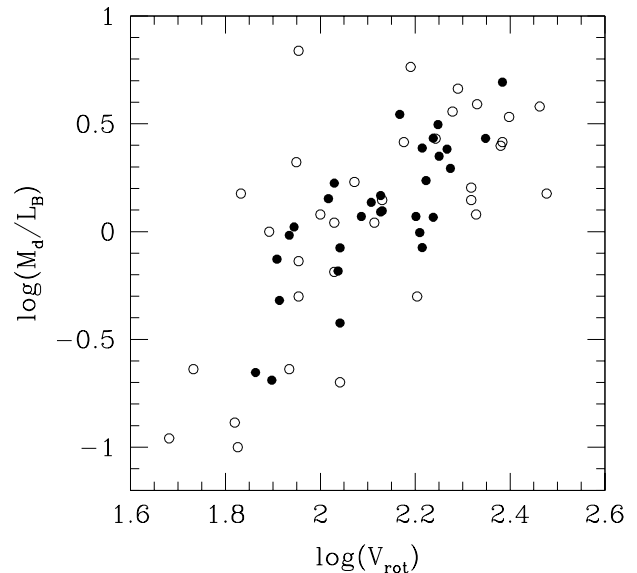


FIG. 3.—The log-log plot of M_d/L_B vs. the observed asymptotic rotation velocity for the sample galaxies (filled circles) compared with the previous sample of field galaxies (open circles) (Paper 2). Here M_d is the total mass of the stellar disk determined from the MOND fit.

M/L_B values given here with the results for the earlier sample, although the range in M/L_B and the scatter about the correlation with V_r is smaller for the Ursa Major sample.

More revealing is the relation between the implied stellar M_d/L_B and the reddening-corrected $B-V$ color index for those 17 sample galaxies (Table 2) with cataloged color-index data (de Vaucouleurs et al. 1991). In Figure 4 this is compared again with the previous sample (there are similar trends with $B-R$ and $B-K'$). Also shown on this plot is the predicted relation between the mass-to-blue light ratio and $B-V$ color from the old galaxy evolution models of Larsen & Tinsley (1978); these predicted properties are those of a population of stars evolved for 10^{10} years with various prescriptions for a monotonically decreasing star formation rate. Although modern galaxy evolution programs are more sophisticated (e.g., Worthey 1994) and include additional parameters (such as the effect of varying metallicity), the overall trends of M/L with color are the same. Here, as previously, the clear trend of increasing M_d/L_B with redness matches that of the model. The evident agreement, not only in form but also in amplitude, is somewhat fortuitous, but it does indicate that the implied MOND M_d/L_B values are astrophysically plausible and consistent with stellar population synthesis models.

It should be recalled that the mass of the stellar disk is the only free parameter in these rotation curve fits. As emphasized in Paper 2, all inadequacies in the data (dispersion in distance, deviations from circular motion, uncertainties introduced by warping or errors in inclination, the unknown contribution of molecular gas to the mass distribution, etc.) are absorbed by this one parameter. In view of this, it is quite striking that the implied mass-to-light ratios have a characteristic value of about 1 in the near-infrared (with small scatter), and in the B band have a dependence with color that is understandable in terms of population synthesis models. This lends support not only to MOND but also to the assumptions underlying this procedure (such as the constancy of M/L in a single galaxy and

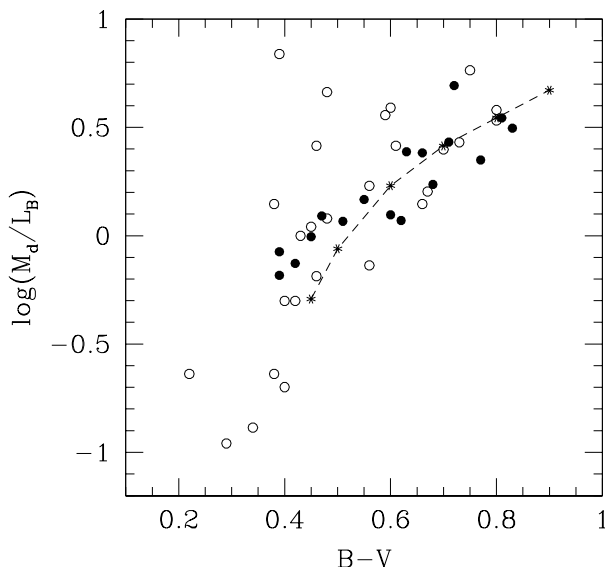


FIG. 4.—The \log of M_d/L_B of sample galaxies (solid circles) vs. the reddening-corrected $B-V$ color from the Third Reference Catalogue (de Vaucouleurs et al. 1991) compared with the previous sample of field galaxies (open circles) (Paper 2). Also shown is the theoretical M/L_B vs. $B-V$ from population synthesis models of Larsen & Tinsley (1978) (dashed line).

the absence of a significant contribution to the surface density by molecular gas that is distributed differently from the stars). In fact, the implied constancy of M_d/L_K elevates the MOND fits to these rotation curves to the level of actual predictions. If one assumes a mass-to-light ratio of about 0.9 in the near-infrared, then with modified dynamics the rotation curve derived from the mean radial distribution of near-infrared emission, when combined with the directly observed gas distribution, would be consistent in most cases with the observed rotation curve, to considerable precision. The same would be true if one used the measured $B-V$ color of a galaxy to estimate M_d/L_B from the Larson and Tinsley population synthesis models. This removes all free parameters, and the rotation curve can be directly calculated from the observed distribution of matter.

5. THE TULLY-FISHER RELATION

Modified dynamics implies a mass-rotation velocity relationship for galaxies that is exact (Milgrom 1983a); it is the MOND equivalent of Kepler's third law in the limit of low acceleration. From equations (2) and (3), it is evident that as the radius becomes large,

$$V^4 = GM_t a_0, \quad (4)$$

where M_t is the total mass of the galaxy, the mass in gas in addition to the stellar disk (i.e., $M_t = M_d + M_g$). This then leads to an observed luminosity-rotation velocity relation (the Tully-Fisher relation) of the form

$$L = (Ga_0 \langle M_t/L \rangle)^{-1} V^4, \quad (5)$$

where $\langle M_t/L \rangle$ is the mean total mass-to-light ratio in the particular band. Expressed as a $\log L$ versus $\log V$ relation, the TF relation in a given color band predicted by MOND becomes

$$\log L = a \log V + b, \quad (6)$$

where $a = 4$ (assuming no systematic variation of M_t/L with V) and $b = -8.2 - \log \langle M_t/L \rangle$; here $\langle M_t/L \rangle$ is expressed in solar units, and we take $a_0 = 1.2 \times 10^{-8} \text{ cm s}^{-2}$, as found in Paper 1. The total mass-to-near-infrared luminosity ratio is given in column (6) of Table 2. Here it is found that for the total sample $\langle M_t/L_K \rangle = 1.2 \pm 0.56$, which means that $b = 8.28$. Note that MOND predicts not only the slope of the logarithmic TF relation but also the intercept.

The observed TF relation in the K' band is shown in Figure 5, where the luminosity and rotation velocity are taken directly from Table 1. A least-square fit, also shown on the plot, gives $a = 3.91 \pm 0.18$ and $b = -8.17 \pm 0.39$, in agreement with the MOND prediction. This is also consistent with a previous determination of the H -band ($1.6 \mu\text{m}$) TF relation for Ursa Major galaxies by Peletier & Willner (1993), who found a slope of 4.08 ± 0.24 . The intrinsic scatter in the TF relation can only arise from the intrinsic scatter in M_t/L_k . Leaving out the most extreme point, UGC 6446 (which, as noted above, may be a foreground object), this is found to be 37%, in agreement with the scatter in the observed K' -band TF relation.

The rotation velocity in Figure 5 is that at the outermost reliable point of the rotation curve and may not correspond to the asymptotic circular velocity, particularly in galaxies in which the outermost centripetal accelerations are greater than a_0 and in the low surface brightness galaxies with

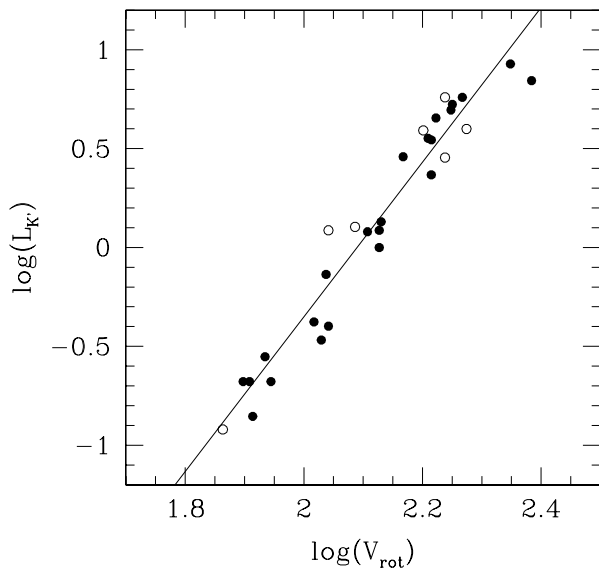


FIG. 5.—The log-log plot of the K' -band luminosity ($10^{10} L_{\odot}$) vs. the observed asymptotic rotation velocity (the K' -band Tully-Fisher relation) for the 30 sample galaxies. The unshaded points are galaxies with perturbed velocity fields. For the total sample, a least-squares fit yields $\log L = (3.91 \pm 0.18) \log V - (8.17 \pm 0.39)$, shown by the solid line.

rotation curves still rising at the last point. Verheijen (1997) has noted that by selecting only those galaxies in the Ursa Major sample in which the rotation curve has reached an asymptotically constant value, and by taking this asymptotic value for the velocity coordinate in the TF relation (as opposed to a global profile width or the peak rotation velocity), the scatter in the TF relation is greatly reduced and the slope is 4 (see also Broeils 1992; Rhee 1996; McGaugh & de Blok 1998a). This is precisely the expectation deduced from MOND, where it is the constant rotation velocity at large distances from the visible galaxy, which correlates exactly with mass (eq. [4]). Verheijen further notes that in this highly selected subsample of 15 galaxies, the scatter in the observed near-infrared TF relation is consistent with the observational scatter; that is to say, no intrinsic scatter in the TF relation can be detected. This is also consistent with MOND, in which the mass-velocity relation is exact; the only source of intrinsic scatter is the M/L , which in the near infrared may be quite small.

Twelve of the galaxies in this sample are in the low surface brightness category as defined by Tully & Verheijen (1997); these are mostly the lower luminosity objects in Figure 5, although there is some overlap in luminosity with objects of high surface brightness. It should be noted that these LSB galaxies lie on the same TF relation defined by the high surface brightness galaxies. This fact, which has been noticed by Zwaan et al. (1995), is an inevitable aspect of MOND, where the TF relation is absolute (McGaugh & de Blok 1998b). Dark halo models, on the other hand, require some contrived coupling of parameters to reproduce this observation (McGaugh & de Blok 1998a).

6. CONCLUSIONS

This sample of galaxies in the Ursa Major cluster, combined with those of Paper 2 and the low surface brightness galaxies analyzed by McGaugh & de Blok (1998b), provide a total sample of about 80 spiral galaxies with rotation curves measured in neutral hydrogen for which the predict-

ed MOND rotation curves have been calculated. Because of the systematic effects, the usual statistical tests of goodness of fit are not entirely appropriate in assessing these rotation curve fits, but qualitatively one would say that in only five or six cases out of this 80 is the rotation curve predicted by MOND from the observed distribution of light and gas noticeably different from the observed rotation curve. In the present sample, NGC 4389 and UGC 6973 should be included in this category. For these objects there is usually an obvious problem with the observed rotation curve or its use as a tracer of the radial force distribution. In other cases, one might question the measured surface brightness distribution as a precise tracer of the stellar mass distribution (for UGC 6973, for example). For about 30 galaxies, the MOND rotation curve reproduces the general shape of the observed curve and accounts for the magnitude of the conventional mass discrepancy with a reasonable mass-to-light ratio (NGC 3877, 4013, and 4138 would fall into this category). In fully half of the objects considered, the MOND rotation curve reproduces the observed curve with considerable precision (as for NGC 4157 and UGC 6399, 6667, and 6917 in the present sample).

Unlike the previous samples, the galaxies considered here are optically selected and form a complete and homogeneous sample. Because selection does not depend primarily on neutral hydrogen richness and extent, these galaxies have a wider range of properties than those in Papers 1 and 2. For example, in a number of these objects the observed rotation curve does not extend far beyond the optical disk into the regime where the discrepancy is large. This is a positive aspect of this sample, since certain general predictions of MOND are seen to be verified; the discrepancy between the Newtonian and observed rotation curve is seen to be small in objects with high centripetal accelerations at the last measured point of the rotation curve, as MOND predicts. In regions where the internal acceleration is low (in the extended rotation curves of high surface brightness galaxies, as in the previous samples), MOND predicts the observed large discrepancy. It should be noted that some of the best fits are achieved for the low surface brightness galaxies where the discrepancy is largest. This is precisely what one would expect from MOND, since these objects lie entirely in the low acceleration limit of the theory, in the deep MOND limit, where there is no uncertainty arising from the unknown function $\mu(x)$ in equation (2) (see also McGaugh & de Blok 1998b).

The range of M/L is generally reasonable and is consistent, in the blue, with population synthesis models. When near-infrared photometry is available, as for this sample, there is remarkably little variation in the fitted M/L of the stellar component, on the order of 30%. When one considers that this is the only free parameter in the fits and will reflect all uncertainties (such as the real dispersion in distance), the results here are consistent with a effectively constant value of the M/L in the near-infrared for spiral galaxies. Assigning the same near-infrared M/L to all galaxies then makes the MOND rotation curves true predictions, without free parameters.

The predictive power of MOND, at least with respect to galaxy rotation curves and the TF relation, is well established. It has been difficult to compare this in a fair way with dark matter halos because, until recently, the dark halo hypotheses have had essentially no predictive power. The exercise has been one of fitting dark matter halos with an

assumed density distribution to the observed rotation curve in order to estimate halo and disk parameters. With at least three free parameters available (disk M/L , halo core radius, and density normalization), essentially any observed rotation curve can be reproduced, as in the analysis of Ursa Major galaxies by Verheijen (1997).

In the last several years, this has changed as the result of the further development of cosmological N -body codes with large numbers of particles and high spatial resolution. It has become evident that in simulations in which the initial spectrum of density fluctuations is that of cold dark matter (CDM), a characteristic form for the radial mass distribution of virialized halos arises (Dubinsky & Carlberg 1991; Navarro, Frenk, & White 1996; Cole & Lacey 1996). This characteristic form is distinguished by a singular density distribution, a density that continues to increase as $1/r$ into the origin. This density law can be parameterized by the Hernquist model (Hernquist 1990; Dubinsky & Carlberg 1991) or by an alternative model suggested by Navarro et al. (1996) that has essentially the same form in the regime where galaxy rotation curves are actually measured. Although these singular halos can produce acceptable fits to the rotation curves of high luminosity, high surface brightness galaxies (Sanders & Begeman 1994), they generally fail in low surface brightness dwarfs (Flores & Primack 1994; Moore 1994). Significantly, Navarro et al. (1996) have demonstrated that given the mass or velocity scaling of a halo, the degree of central concentration (or the halo length scale) is determined by the cosmology. McGaugh & de Blok (1998b) show that such constrained halos dramatically fail to reproduce the rotation curves of the low surface brightness galaxies for plausible cosmologies; it is impossible to match the gradual rise in the observed rotation curve in the inner region with the asymptotic velocity at larger radii; the singular density distribution produces a rotation curve that rises far too steeply.

The predicted mass-velocity relation for the CDM halos (not considering that the observed correlation is with the luminosity of the baryonic component) is closer to $M \propto V^3$

(White 1997), while $M \propto V^4$ for MOND; again, a clearly distinct prediction. In this sense also, MOND is successful when one considers the correlation between the asymptotic flat rotation velocity and the luminosity (Verheijen 1997). Therefore, on this very basic phenomenological level, one can only conclude that MOND works where dark matter, at least the presently favored form of dark matter, does not.

It is sometimes argued that MOND is “designed” to fit rotation curves, and so it is no surprise that it works so well on this scale. It is true that MOND is, in some sense, designed to reproduce asymptotically flat rotation curves and a TF relation of the form $L \propto V^4$. But it is by no means evident that the variety of detailed shapes of rotation curves exhibited by the total sample of 80 galaxies so far considered could be so precisely reproduced by using MOND to calculate the radial force from the observed distribution of detectable matter. MOND works well throughout the entire galaxy, not just where the rotation attains its asymptotic constant value, and it was in no sense designed to do this. Using MOND, Milgrom *predicted* that the discrepancy between the observed curve and the Newtonian rotation curve should be small in regions of high surface brightness and large in galaxies of low surface brightness, even before such galaxies were discovered. These predictions are clearly verified in the sample of galaxies considered here, which includes both types of systems. It is this inherent simplicity and predictive power that gives the idea its continued impact in spite of the absence of a solid theoretical basis for MOND. The detailed shape and amplitude of a rotation curve can be calculated from the observed distribution of detectable matter with no free parameters by assuming a fixed value of M/L of about 1 in the near-infrared. What more could one expect from a theory of gravity? Because of this, it is justifiable to claim that MOND, at the present time, is epistemologically superior to the dark matter hypothesis.

We are very grateful to M. Milgrom and S. S. McGaugh for very helpful comments on this manuscript.

REFERENCES

- Begeman, K. G. 1987, Ph.D. thesis, Kapteyn Institute
 Begeman, K. G., Broeils, A. H., & Sanders, R. H. 1991, MNRAS, 249, 523 (Paper 1)
 Broeils, A. H. 1992, Ph.D. thesis, Kapteyn Institute
 Cole, S. M., & Lacey, C. G. 1996, MNRAS, 281, 716
 de Vaucouleurs, G., et al. 1991, Third Reference Catalog of Bright Galaxies (New York: Springer)
 Dubinsky, J., & Carlberg, R. G. 1991, ApJ, 378, 496
 Flores, R., & Primack, J. R. 1994, ApJ, 427, L1
 Hernquist, L. 1990, ApJ, 356, 359
 Larson, R. B., & Tinsley, B. M. 1978, ApJ, 219, 46
 McGaugh, S. S., & de Blok, W. J. G. 1998a, ApJ, 499, 41
 ———. 1998b, ApJ, 499, 66
 Milgrom, M. 1983a, ApJ, 270, 365
 ———. 1983b, ApJ, 270, 371
 ———. 1983c, ApJ, 270, 384
 Moore, B. 1994, Nature, 370, 629
 Navarro, J. F., Frenk, C. S., & White, S. D. M. 1996, ApJ, 462, 563
 Peletier, R. F., & Willner, S. P. 1993, ApJ, 418, 626
 Rhee, M.-H. 1996, Ph.D. thesis, Kapteyn Institute
 Sanders, R. H. 1996, ApJ, 473, 117 (Paper 2)
 Sanders, R. H., & Begeman, K. G. 1994, MNRAS, 266, 360
 Tully, R. B., & Verheijen, M. A. W. 1997, ApJ, 484, 145
 Tully, R. B., Verheijen, M. A. W., Pierce, M. J., Huang, J.-S., & Wainscoat, R. 1996, AJ, 112, 2471
 Verheijen, M. A. W. 1997, Ph.D. thesis, Kapteyn Institute
 White, S. D. M. 1997, in Galaxy Scaling Relations, ed. L. N. da Costa & A. Renzini (New York: Springer), 3
 Worthey, G. 1994, ApJS, 95, 107
 Zwaan, M. A., van der Hulst, J. M., de Blok, W. J. G., & McGaugh, S. S. 1995, MNRAS, 273, L35